

An exactly solvable model for the dynamics of two spin- $\frac{1}{2}$ particles embedded in separate spin star environments

This article has been downloaded from IOPscience. Please scroll down to see the full text article.

2009 J. Phys. A: Math. Theor. 42 315301

(<http://iopscience.iop.org/1751-8121/42/31/315301>)

View [the table of contents for this issue](#), or go to the [journal homepage](#) for more

Download details:

IP Address: 171.66.16.155

The article was downloaded on 03/06/2010 at 08:02

Please note that [terms and conditions apply](#).

An exactly solvable model for the dynamics of two spin- $\frac{1}{2}$ particles embedded in separate spin star environments

Yamen Hamdouni¹

School of Physics, University of KwaZulu-Natal, Westville Campus, Durban 4001, South Africa

E-mail: hamdouniyamen@gmail.com

Received 15 February 2009, in final form 29 May 2009

Published 13 July 2009

Online at stacks.iop.org/JPhysA/42/315301

Abstract

Exact analytical results for the dynamics of two interacting qubits, each of which is embedded in its own spin star bath, are presented. The time evolution of the concurrence and the purity of the two-qubit system are investigated for finite and infinite numbers of environmental spins. The effect of qubit–qubit interactions on the steady state of the central system is investigated.

PACS numbers: 03.65.Yz, 03.67.Lx, 73.21.La, 75.10.Jm

(Some figures in this article are in colour only in the electronic version)

1. Introduction

Exactly solvable models play a very useful role in various fields of physics. They help to improve our understanding of physical processes and allow us to gain more insight into complicated phenomena that take place in nature [1]. One may recall, for instance, the usefulness of exactly solvable models such as the harmonic oscillator, the nuclear shell model and the Ising model, to name a few. From a practical point of view, exactly solvable models serve as a very convenient tool for testing the accuracy of numerical algorithms, often used in the study of problems that cannot be analytically solved, due to the complexity of the systems under investigation. This is usually the case in the field of open quantum systems, where one faces uncontrolled degrees of freedom of the environments.

Let us recall that realistic quantum systems are influenced by their surrounding through, in general, complicated coupling interactions, leading them to lose their coherences [2]. This is referred to as the decoherence process, which is the main obstacle to quantum information processing [3–5]. The latter can be improved by exploiting the entanglement, i.e. the nonlocal quantum correlations that exist between quantum systems [6]. This resource has no classical analogue, and it turns out to be of great importance in quantum teleportation and quantum

¹ Permanent Address: Institut de Physique, Université Mentouri de Constantine, Constantine, Algeria.

computing [7–12]. It is worth mentioning that over the last few years, many proposals have been made for the implementation of quantum information processing. Solid-state systems are very promising [13, 14] and have been the subject of many investigations. Much attention was devoted to the study of the decoherence and the entanglement of simple qubit systems that are coupled to spin environments [15–19]. Thus, new exactly solvable models describing the dynamics of qubits within spin baths are highly welcome. Recently, the spin star configuration, initially proposed in [20], has been extensively investigated [21–25]. An exact treatment of the dynamics of two qubits coupled to the common spin star bath via XY interactions is presented in [26, 27]. In this paper, we propose to investigate analytically the dynamics when the two qubits interact with separate spin star baths.

This paper is organized as follows. In section 2, the model Hamiltonian is introduced. In section 3, we present a detailed derivation of the time evolution operator. In section 4, we investigate the dynamics of the qubits at a finite number of the environmental spins for some particular initial conditions. In section 5, we study the case of an infinite number of spins within the environments. Section 6 is devoted to the second-order master equation, where the short-time behaviour is explored. We end the paper with a short summary.

2. Model

2.1. Hamiltonian

The system under study consists of two two-level systems (e.g. spin- $\frac{1}{2}$ particles), each of which is embedded in its own spin star environment composed of N spin- $\frac{1}{2}$. The central particles interact with each other through an Ising interaction; the corresponding coupling constant is equal to 4δ , where the factor 4 is introduced for later convenience. We shall assume that each qubit couples to its environment via Heisenberg XY interaction whose coupling constant, α , is scaled by \sqrt{N} in order to ensure good thermodynamic behaviour. From here on, the spin environments will be denoted by B_1 and B_2 .

The Hamiltonian for the composite system has the form

$$H = H_0 + H_{S_1 B_1} + H_{S_2 B_2}, \quad (1)$$

where

$$H_0 = 4\delta S_z^1 S_z^2, \quad (2)$$

and

$$H_{S_i B_i} = \frac{\alpha}{\sqrt{N}} \left(S_+^i \sum_{k=1}^N S_-^{ik} + S_-^i \sum_{k=1}^N S_+^{ik} \right), \quad i = 1, 2. \quad (3)$$

Here \vec{S}^1 and \vec{S}^2 denote the spin operators corresponding to the central qubits, whereas \vec{S}^{ik} denotes the spin operator corresponding to the k th particle within the i th environment. Introducing the total spin operators $\vec{J} = \sum_{k=1}^N \vec{S}^{1k}$ and $\vec{J} = \sum_{k=1}^N \vec{S}^{2k}$, one can rewrite the full Hamiltonian as

$$H = 4\delta S_z^1 S_z^2 + \frac{\alpha}{\sqrt{N}} (S_+^1 J_- + S_-^1 J_+ + S_+^2 J_- + S_-^2 J_+). \quad (4)$$

The dynamics of the two-qubit system is fully described by its density matrix $\rho(t)$ obtained by tracing the time-dependent total density matrix $\rho_{\text{tot}}(t)$, describing the composite system, with respect to the environmental degrees of freedom:

$$\rho(t) = \text{tr}_{B_1+B_2}[\rho_{\text{tot}}(t)] = \text{tr}_{B_1+B_2}[\mathbf{U}(t)\rho_{\text{tot}}(0)\mathbf{U}^\dagger(t)]. \quad (5)$$

In the above, $\mathbf{U}(t)$ and $\rho_{\text{tot}}(0)$ designate the time evolution operator and the initial total density matrix respectively.

2.2. Initial conditions

At $t = 0$, the central qubits are assumed to be uncoupled from environments; the latter are in thermal equilibrium at infinite temperature. This means that the initial total density matrix can be written as

$$\rho_{\text{tot}}(0) = \rho(0) \otimes \frac{\mathbf{1}}{2^N} \otimes \frac{\mathbf{1}}{2^N}, \quad (6)$$

where $\rho(0)$ is the initial density matrix of the two-qubit system and $\mathbf{1}$ is the unit matrix on the space $\mathbb{C}^{2^{\otimes N}}$. The former can be expressed as

$$\rho(0) = \sum_{k,\ell} \rho_{k\ell}^0 |\chi_k\rangle \langle \chi_\ell|, \quad (7)$$

where $|\chi_\ell\rangle \in \{|--\rangle, |-\rangle, |+\rangle, |++\rangle\}$ for $\ell = \overline{1, 4}$.

Recall that the basis state vectors of $\mathbb{C}^{2^{\otimes N}}$ are given by $|j, m\rangle$, with $\kappa \leq j \leq N/2$ ($\kappa = 0$ for N even and $\kappa = 1/2$ for N odd), and $-j \leq m \leq j$ ($\hbar = 1$). The degeneracy corresponding to each value j of the collective spin operator is equal to [28]

$$v(N, j) = \binom{N}{N/2 - j} - \binom{N}{N/2 - j - 1}. \quad (8)$$

Then the time-dependent reduced density matrix can be expressed as

$$\rho(t) = 2^{-2N} \sum_{k,\ell} \rho_{k\ell}^0 \sum_{j,m} \sum_{r,s} v(N, j) v(N, r) \langle j, r, m, s | \mathbf{U}(t) | \chi_k \rangle \langle \chi_\ell | \mathbf{U}^\dagger(t) | j, r, m, s \rangle, \quad (9)$$

where $|j, r, m, s\rangle = |j, m\rangle \otimes |r, s\rangle$. Hence, our task reduces to finding the exact form of the matrix elements of the time evolution operator; this makes the subject of the following section.

3. Derivation of the exact form of the time evolution operator

The Hamiltonian of our model does not depend on time. Consequently, the time evolution operator is simply given by $\mathbf{U}(t) = \exp(-iHt)$, which can be expanded in Taylor series as

$$\mathbf{U}(t) = \sum_{n=0}^{\infty} \frac{(-1)^n t^{2n}}{(2n)!} (H)^{2n} - i \sum_{n=0}^{\infty} \frac{(-1)^n t^{2n+1}}{(2n+1)!} (H)^{2n+1}. \quad (10)$$

In order to derive analytical expressions for even and odd powers of the total Hamiltonian, we note that H_0 anticommutes with $H_{S_1 B_1} + H_{S_2 B_2}$:

$$[H_0, H_{S_1 B_1} + H_{S_2 B_2}]_+ = 0. \quad (11)$$

This can easily be shown using the following properties of spin- $\frac{1}{2}$ operators: $S_z S_\pm = \pm S_\pm$ and $S_\pm S_z = \mp S_\pm$.

Furthermore, taking into account that $H_0^{2n} \equiv \delta^{2n}$, we find that for $n \geq 0$,

$$H^{2n} = \sum_{\ell=0}^n \binom{n}{\ell} (H_{S_1 B_1} + H_{S_2 B_2})^{2\ell} \delta^{2(n-\ell)}. \quad (12)$$

Hence, since $H_{S_1 B_1}$ commutes with $H_{S_2 B_2}$, we only need to know the expressions of powers of each of the latter operators. These are shown in appendix A.

It follows, using equations (A.1)–(A.4), that

$$\begin{aligned} (H_{S_1 B_1} + H_{S_2 B_2})^{2\ell} &= \sum_{k=0}^{\ell} \binom{2\ell}{2k} H_{S_1 B_1}^{2k} H_{S_2 B_2}^{2(\ell-k)} + \sum_{k=0}^{\ell-1} \binom{2\ell}{2k+1} H_{S_1 B_1}^{2k+1} H_{S_2 B_2}^{2(\ell-k)-1} \\ &= \left(\frac{\alpha}{\sqrt{N}}\right)^{2\ell} \left[\sum_{k=0}^{\ell} \binom{2\ell}{2k} D_{\ell k} + \sum_{k=0}^{\ell-1} \binom{2\ell}{2k+1} L_{\ell k} \right]. \end{aligned} \quad (13)$$

where

$$D_{\ell k} = \text{diag}[(J_+ J_-)^k (\mathcal{J}_+ \mathcal{J}_-)^{\ell-k}, (J_+ J_-)^k (\mathcal{J}_- \mathcal{J}_+)^{\ell-k}, (J_- J_+)^k (\mathcal{J}_+ \mathcal{J}_-)^{\ell-k}, (J_- J_+)^k (\mathcal{J}_- \mathcal{J}_+)^{\ell-k}] \quad (14)$$

and

$$L_{\ell k} = \text{antidiag}[J_+ \mathcal{J}_+ (J_- J_+)^k (\mathcal{J}_- \mathcal{J}_+)^{\ell-k-1}, J_+ \mathcal{J}_- (J_- J_+)^k (\mathcal{J}_+ \mathcal{J}_-)^{\ell-k-1}, J_- \mathcal{J}_+ (J_+ J_-)^k (\mathcal{J}_- \mathcal{J}_+)^{\ell-k-1}, J_- \mathcal{J}_- (J_+ J_-)^k (\mathcal{J}_+ \mathcal{J}_-)^{\ell-k-1}]. \quad (15)$$

Afterwards, it is straightforward to show that

$$(H_{S_1 B_1} + H_{S_2 B_2})^{2\ell} = \left(\frac{\alpha}{\sqrt{N}} \right)^{2\ell} \times \begin{pmatrix} F_1^+ & 0 & 0 & J_+ \mathcal{J}_+ \frac{F_4^-}{\sqrt{J_- J_+ \mathcal{J}_- \mathcal{J}_+}} \\ 0 & F_2^+ & J_+ \mathcal{J}_- \frac{F_3^-}{\sqrt{J_- J_+ \mathcal{J}_+ \mathcal{J}_-}} & 0 \\ 0 & J_- \mathcal{J}_+ \frac{F_2^-}{\sqrt{J_+ J_- \mathcal{J}_- \mathcal{J}_+}} & F_3^+ & 0 \\ J_- \mathcal{J}_- \frac{F_1^-}{\sqrt{J_+ J_- \mathcal{J}_+ \mathcal{J}_-}} & 0 & 0 & F_4^+ \end{pmatrix}, \quad (16)$$

where

$$F_1^\pm = \frac{1}{2} [(\sqrt{J_+ J_-} + \sqrt{\mathcal{J}_+ \mathcal{J}_-})^{2\ell} \pm (\sqrt{J_+ J_-} - \sqrt{\mathcal{J}_+ \mathcal{J}_-})^{2\ell}], \quad (17)$$

$$F_2^\pm = \frac{1}{2} [(\sqrt{J_+ J_-} + \sqrt{\mathcal{J}_- \mathcal{J}_+})^{2\ell} \pm (\sqrt{J_+ J_-} - \sqrt{\mathcal{J}_- \mathcal{J}_+})^{2\ell}], \quad (18)$$

$$F_3^\pm = \frac{1}{2} [(\sqrt{J_- J_+} + \sqrt{\mathcal{J}_+ \mathcal{J}_-})^{2\ell} \pm (\sqrt{J_- J_+} - \sqrt{\mathcal{J}_+ \mathcal{J}_-})^{2\ell}], \quad (19)$$

$$F_4^\pm = \frac{1}{2} [(\sqrt{J_- J_+} + \sqrt{\mathcal{J}_- \mathcal{J}_+})^{2\ell} \pm (\sqrt{J_- J_+} - \sqrt{\mathcal{J}_- \mathcal{J}_+})^{2\ell}]. \quad (20)$$

Inserting equation (16) into equation (12) yields

$$H^{2n} = \frac{1}{2} \times \begin{pmatrix} (\mathcal{M}_1^+)^n + (\mathcal{M}_1^-)^n & 0 & 0 & \Gamma_{4n} \\ 0 & (\mathcal{M}_2^+)^n + (\mathcal{M}_2^-)^n & \Gamma_{3n} & 0 \\ 0 & \Gamma_{2n} & (\mathcal{M}_3^+)^n + (\mathcal{M}_3^-)^n & 0 \\ \Gamma_{1n} & 0 & 0 & (\mathcal{M}_4^+)^n + (\mathcal{M}_4^-)^n \end{pmatrix}, \quad (21)$$

where

$$\Gamma_{1n} = J_- \mathcal{J}_- \frac{(\mathcal{M}_1^+)^n - (\mathcal{M}_1^-)^n}{\sqrt{J_+ J_- \mathcal{J}_+ \mathcal{J}_-}}, \quad \Gamma_{2n} = J_- \mathcal{J}_+ \frac{(\mathcal{M}_2^+)^n - (\mathcal{M}_2^-)^n}{\sqrt{J_+ J_- \mathcal{J}_- \mathcal{J}_+}}, \quad (22)$$

$$\Gamma_{3n} = J_+ \mathcal{J}_- \frac{(\mathcal{M}_3^+)^n - (\mathcal{M}_3^-)^n}{\sqrt{J_- J_+ \mathcal{J}_+ \mathcal{J}_-}}, \quad \Gamma_{4n} = J_+ \mathcal{J}_+ \frac{(\mathcal{M}_4^+)^n - (\mathcal{M}_4^-)^n}{\sqrt{J_- J_+ \mathcal{J}_- \mathcal{J}_+}}, \quad (23)$$

with

$$\mathcal{M}_1^\pm = \delta^2 + \frac{\alpha^2}{N} (\sqrt{J_+ J_-} \pm \sqrt{\mathcal{J}_+ \mathcal{J}_-})^2, \quad (24)$$

$$\mathcal{M}_2^\pm = \delta^2 + \frac{\alpha^2}{N} (\sqrt{J_+ J_-} \pm \sqrt{\mathcal{J}_- \mathcal{J}_+})^2, \quad (25)$$

$$\mathcal{M}_3^\pm = \delta^2 + \frac{\alpha^2}{N} (\sqrt{J_- J_+} \pm \sqrt{\mathcal{J}_+ \mathcal{J}_-})^2, \tag{26}$$

$$\mathcal{M}_4^\pm = \delta^2 + \frac{\alpha^2}{N} (\sqrt{J_- J_+} \pm \sqrt{\mathcal{J}_- \mathcal{J}_+})^2. \tag{27}$$

The matrix elements of H^{2n+1} can readily be obtained by multiplying the right-hand side of (21) with H . The results are also presented in appendix A.

Having derived the explicit expressions of powers of the total Hamiltonian, we can easily verify that the elements of the time evolution operator, obtained by inserting equations (21) and (A.5)–(A.28) into equation (10), are given by

$$U_{11}(t) = \frac{1}{2} \left\{ \cos(t\sqrt{\mathcal{M}_1^+}) + \cos(t\sqrt{\mathcal{M}_1^-}) - i\delta \left[\frac{\sin(t\sqrt{\mathcal{M}_1^+})}{\sqrt{\mathcal{M}_1^+}} + \frac{\sin(t\sqrt{\mathcal{M}_1^-})}{\sqrt{\mathcal{M}_1^-}} \right] \right\}, \tag{28}$$

$$U_{21}(t) = -\mathcal{J}_- \frac{i\alpha/2}{\sqrt{N\mathcal{J}_+\mathcal{J}_-}} \left\{ \frac{\sqrt{J_+J_-} + \sqrt{\mathcal{J}_+\mathcal{J}_-}}{\sqrt{\mathcal{M}_1^+}} \sin(t\sqrt{\mathcal{M}_1^+}) - \frac{\sqrt{J_+J_-} - \sqrt{\mathcal{J}_+\mathcal{J}_-}}{\sqrt{\mathcal{M}_1^-}} \sin(t\sqrt{\mathcal{M}_1^-}) \right\}, \tag{29}$$

$$U_{31}(t) = -J_- \frac{i\alpha/2}{\sqrt{N\mathcal{J}_+J_-}} \left\{ \frac{\sqrt{J_+J_-} + \sqrt{\mathcal{J}_+\mathcal{J}_-}}{\sqrt{\mathcal{M}_1^+}} \sin(t\sqrt{\mathcal{M}_1^+}) + \frac{\sqrt{J_+J_-} - \sqrt{\mathcal{J}_+\mathcal{J}_-}}{\sqrt{\mathcal{M}_1^-}} \sin(t\sqrt{\mathcal{M}_1^-}) \right\}, \tag{30}$$

$$U_{41}(t) = J_- \mathcal{J}_- \frac{1}{2\sqrt{J_+J_- \mathcal{J}_+\mathcal{J}_-}} \left\{ \cos(t\sqrt{\mathcal{M}_1^+}) - \cos(t\sqrt{\mathcal{M}_1^-}) - i\delta \left[\frac{\sin(t\sqrt{\mathcal{M}_1^+})}{\sqrt{\mathcal{M}_1^+}} - \frac{\sin(t\sqrt{\mathcal{M}_1^-})}{\sqrt{\mathcal{M}_1^-}} \right] \right\}, \tag{31}$$

$$U_{22}(t) = \frac{1}{2} \left\{ \cos(t\sqrt{\mathcal{M}_2^+}) + \cos(t\sqrt{\mathcal{M}_1^-}) + i\delta \left[\frac{\sin(t\sqrt{\mathcal{M}_2^+})}{\sqrt{\mathcal{M}_2^+}} + \frac{\sin(t\sqrt{\mathcal{M}_1^-})}{\sqrt{\mathcal{M}_1^-}} \right] \right\}, \tag{32}$$

$$U_{12}(t) = -\mathcal{J}_+ \frac{i\alpha/2}{\sqrt{N\mathcal{J}_-\mathcal{J}_+}} \left\{ \frac{\sqrt{J_+J_-} + \sqrt{\mathcal{J}_-\mathcal{J}_+}}{\sqrt{\mathcal{M}_2^+}} \sin(t\sqrt{\mathcal{M}_2^+}) - \frac{\sqrt{J_+J_-} - \sqrt{\mathcal{J}_-\mathcal{J}_+}}{\sqrt{\mathcal{M}_2^-}} \sin(t\sqrt{\mathcal{M}_2^-}) \right\}, \tag{33}$$

$$U_{32}(t) = J_- \mathcal{J}_+ \frac{1}{2\sqrt{J_+J_- \mathcal{J}_-\mathcal{J}_+}} \left\{ \cos(t\sqrt{\mathcal{M}_2^+}) - \cos(t\sqrt{\mathcal{M}_2^-}) + i\delta \left[\frac{\sin(t\sqrt{\mathcal{M}_2^+})}{\sqrt{\mathcal{M}_2^+}} - \frac{\sin(t\sqrt{\mathcal{M}_2^-})}{\sqrt{\mathcal{M}_2^-}} \right] \right\}, \tag{34}$$

$$U_{42}(t) = -J_- \frac{i\alpha/2}{\sqrt{NJ_+J_-}} \left\{ \frac{\sqrt{J_+J_-} + \sqrt{\mathcal{J}_-\mathcal{J}_+}}{\sqrt{\mathcal{M}_2^+}} \sin(t\sqrt{\mathcal{M}_2^+}) + \frac{\sqrt{J_+J_-} - \sqrt{\mathcal{J}_-\mathcal{J}_+}}{\sqrt{\mathcal{M}_2^-}} \sin(t\sqrt{\mathcal{M}_2^-}) \right\}, \quad (35)$$

$$U_{33}(t) = \frac{1}{2} \left\{ \cos(t\sqrt{\mathcal{M}_3^+}) + \cos(t\sqrt{\mathcal{M}_3^-}) + i\delta \left[\frac{\sin(t\sqrt{\mathcal{M}_3^+})}{\sqrt{\mathcal{M}_3^+}} + \frac{\sin(t\sqrt{\mathcal{M}_3^-})}{\sqrt{\mathcal{M}_3^-}} \right] \right\}, \quad (36)$$

$$U_{13}(t) = -J_+ \frac{i\alpha/2}{\sqrt{NJ_-J_+}} \left\{ \frac{\sqrt{\mathcal{J}_+\mathcal{J}_-} + \sqrt{J_-J_+}}{\sqrt{\mathcal{M}_3^+}} \sin(t\sqrt{\mathcal{M}_3^+}) - \frac{\sqrt{\mathcal{J}_+\mathcal{J}_-} - \sqrt{J_-J_+}}{\sqrt{\mathcal{M}_3^-}} \sin(t\sqrt{\mathcal{M}_3^-}) \right\}, \quad (37)$$

$$U_{23}(t) = J_+\mathcal{J}_- \frac{1}{2\sqrt{J_-J_+\mathcal{J}_+\mathcal{J}_-}} \left\{ \cos(t\sqrt{\mathcal{M}_3^+}) - \cos(t\sqrt{\mathcal{M}_3^-}) + i\delta \left[\frac{\sin(t\sqrt{\mathcal{M}_3^+})}{\sqrt{\mathcal{M}_3^+}} - \frac{\sin(t\sqrt{\mathcal{M}_3^-})}{\sqrt{\mathcal{M}_3^-}} \right] \right\}, \quad (38)$$

$$U_{43}(t) = -\mathcal{J}_- \frac{i\alpha/2}{\sqrt{N\mathcal{J}_+\mathcal{J}_-}} \left\{ \frac{\sqrt{\mathcal{J}_+\mathcal{J}_-} + \sqrt{J_-J_+}}{\sqrt{\mathcal{M}_3^+}} \sin(t\sqrt{\mathcal{M}_3^+}) + \frac{\sqrt{\mathcal{J}_+\mathcal{J}_-} - \sqrt{J_-J_+}}{\sqrt{\mathcal{M}_3^-}} \sin(t\sqrt{\mathcal{M}_3^-}) \right\}, \quad (39)$$

$$U_{44}(t) = \frac{1}{2} \left\{ \cos(t\sqrt{\mathcal{M}_4^+}) + \cos(t\sqrt{\mathcal{M}_4^-}) - i\delta \left[\frac{\sin(t\sqrt{\mathcal{M}_4^+})}{\sqrt{\mathcal{M}_4^+}} + \frac{\sin(t\sqrt{\mathcal{M}_4^-})}{\sqrt{\mathcal{M}_4^-}} \right] \right\}, \quad (40)$$

$$U_{24}(t) = -J_+ \frac{i\alpha/2}{\sqrt{NJ_-J_+}} \left\{ \frac{\sqrt{\mathcal{J}_-\mathcal{J}_+} + \sqrt{J_-J_+}}{\sqrt{\mathcal{M}_4^+}} \sin(t\sqrt{\mathcal{M}_4^+}) - \frac{\sqrt{\mathcal{J}_-\mathcal{J}_+} - \sqrt{J_-J_+}}{\sqrt{\mathcal{M}_4^-}} \sin(t\sqrt{\mathcal{M}_4^-}) \right\}, \quad (41)$$

$$U_{34}(t) = -\mathcal{J}_+ \frac{i\alpha/2}{\sqrt{N\mathcal{J}_-\mathcal{J}_+}} \left\{ \frac{\sqrt{\mathcal{J}_-\mathcal{J}_+} + \sqrt{J_-J_+}}{\sqrt{\mathcal{M}_4^+}} \sin(t\sqrt{\mathcal{M}_4^+}) + \frac{\sqrt{\mathcal{J}_-\mathcal{J}_+} - \sqrt{J_-J_+}}{\sqrt{\mathcal{M}_4^-}} \sin(t\sqrt{\mathcal{M}_4^-}) \right\}, \quad (42)$$

$$U_{14}(t) = J_+ \mathcal{J}_+ \frac{1}{2\sqrt{J_- J_+ \mathcal{J}_- \mathcal{J}_+}} \left\{ \cos(t\sqrt{\mathcal{M}_4^+}) - \cos(t\sqrt{\mathcal{M}_4^-}) - i\delta \left[\frac{\sin(t\sqrt{\mathcal{M}_4^+})}{\sqrt{\mathcal{M}_4^+}} - \frac{\sin(t\sqrt{\mathcal{M}_4^-})}{\sqrt{\mathcal{M}_4^-}} \right] \right\}. \quad (43)$$

In the following section, we are going to investigate the time evolution of some measures that quantify the decoherence and the entanglement of the central qubits system.

4. Concurrence and purity evolution

There exist many measures for entanglement. Here we use the concurrence, defined by [29]

$$C(\rho) = \max \left\{ 0, 2 \max[\sqrt{\lambda_i}] - \sum_{i=1}^4 \sqrt{\lambda_i} \right\}, \quad (44)$$

where the quantities λ_i are the eigenvalues of the operator $\rho(t)(\sigma_y \otimes \sigma_y)\rho(t)^*(\sigma_y \otimes \sigma_y)$. The above measure is equal to 1 for maximally entangled states and is equal to 0 for separable states. On the other hand, as is well known, due to the decoherence process, pure states evolve into mixed ones while the degree of mixing of mixed states increases. A suitable measure for decoherence is the purity $P(t)$, given by the trace of the square of the reduced density matrix of the central two-qubit system, that is,

$$P(t) = \text{tr} \rho(t)^2. \quad (45)$$

The above measure is equal to $\frac{1}{4}$ for maximally mixed states and is equal to 1 for pure states.

It turns out that the density matrices corresponding to the initial product states $|\epsilon_1 \epsilon_2\rangle$, where $\epsilon_i \equiv \pm$, are always diagonal. The analysis of the dynamics in this case reveals that if the qubits are prepared in one of the above states, they remain unentangled regardless of the values of N and δ , in contrast to the case of a common bath where entanglement may be generated in the case of the initial product states $|\pm, \mp\rangle$. Furthermore, it is found that for finite values of α , the purity decreases slower with the increase of the interaction strength, δ . This decay is of Gaussian nature, as expected for non-Markovian spin dynamics [19] (see section 6).

The matrix elements of the reduced density matrices corresponding to the states $|e_{\pm}\rangle = \frac{1}{\sqrt{2}}(|-+\rangle \pm |+-\rangle)$ and $|v_{\pm}\rangle = \frac{1}{\sqrt{2}}(|++\rangle \pm |--\rangle)$ are shown in appendix B. The evolution in time of the concurrence and the purity corresponding to the above maximally entangled states is practically the same. This is in clear agreement with [18] where, with a different model Hamiltonian, it is shown that Bell's maximally entangled states all display the same behaviour when the two qubits are located in different spin environments. The author also concluded that if the qubits interact with the same spin bath, then we can distinguish between the behaviour of the concurrence of the states $\frac{1}{\sqrt{2}}(|-+\rangle \pm |+-\rangle)$ on the one hand and that corresponding to the states $\frac{1}{\sqrt{2}}(|++\rangle \pm |--\rangle)$ on the other hand. In [27], we have shown that the singlet state is decoherence free whereas the concurrence of all the other Bell states decays in time. However, we found that the state $|e_+\rangle$ is less sensitive to the effect of the environment than the states $|v_{\pm}\rangle$. This implies a dependence of the behaviour of the concurrence on the relative orientation of the two qubits if they interact with the same bath. The above factor has no effect on the dynamics in the case of separate environments. In what follows, we only present the results obtained for the singlet state.

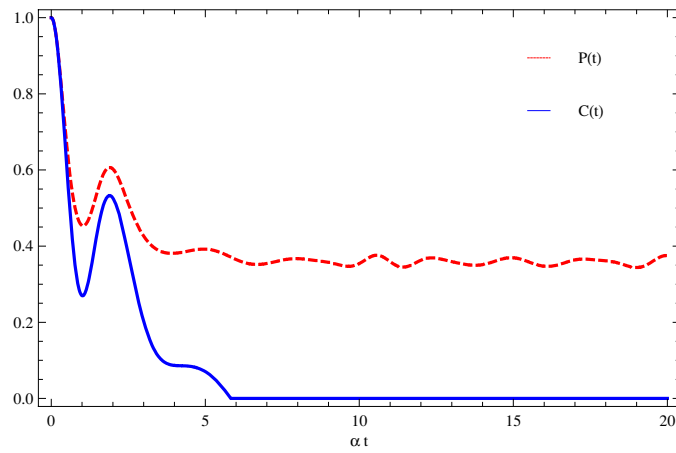


Figure 1. The evolution in time of the concurrence (solid curve) and the purity (dashed curve) corresponding to the singlet state for $\delta = \alpha$ and $N = 10$.

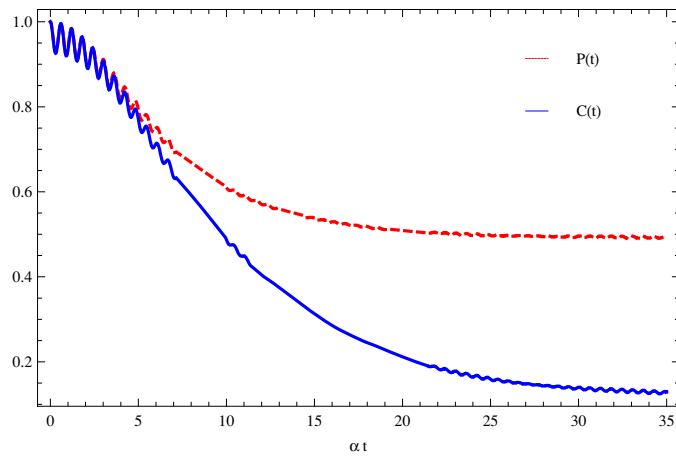


Figure 2. The evolution in time of the concurrence (solid curve) and the purity (dashed curve) corresponding to the singlet state for $\delta = 4\alpha$ and $N = 10$.

It is found that, for fixed δ , the concurrence and the purity saturate as the number of spins increases. This naturally suggests the investigation of the case $N \rightarrow \infty$ (see the following section). In figures 1 and 2 we have plotted the concurrence and the purity, obtained from the analytical solution for, respectively, $\delta = \alpha$ and $\delta = 4\alpha$ with $N = 10$ in both cases. We see that for small values of the coupling constant, the concurrence decays from its initial maximum value $C_{\max} = 1$ and then vanishes at a certain moment of time (i.e. entanglement sudden death [30]). For sufficiently large δ , the purity and the concurrence decay less, displaying fast oscillations. At long times, they converge to certain asymptotic values which increase with the increase of the strength of interaction. Note that it may happen that the concurrence revives at a later time which depends, of course, on the parameters of the model. It is also interesting to mention that at short times, the concurrence and the purity are identical. The intervals at which this occurs are longer for large δ . The investigation of the short-time behaviour will be carried out in section 6 through the solutions of the second-order master equation. Finally let us remark that although we have only considered infinite temperature, we can ensure that

for long-range antiferromagnetic Heisenberg interactions within the baths, low temperatures will have the same effect on decoherence and entanglement of the qubits as strong coupling constants.

5. The case of an infinite number of bath spins

In the limit $N \rightarrow \infty$, the operators $\sqrt{J_{\pm}J_{\mp}/N}$ converge to the positive real random variable r whose probability density function is given by

$$r \mapsto f(r) = 4r e^{-2r^2}, \quad r \geq 0. \quad (46)$$

Indeed, it has been shown in [25, 26] that the operator J_+/\sqrt{N} converges to the complex normal random variable z with the probability density function

$$z \mapsto \frac{2}{\pi} e^{-2|z|^2}. \quad (47)$$

Expressing z in terms of the polar coordinates r and ϕ , i.e., $z = re^{i\phi}$, simply gives $|z|^2 = r^2$. Then integrating the corresponding probability density function over the variable ϕ from 0 to 2π yields

$$\begin{aligned} dP(r) &= f(r) dr = \frac{2}{\pi} \int_0^{2\pi} d\phi r dr e^{-2r^2} \\ &= 4r e^{-2r^2} dr, \end{aligned} \quad (48)$$

from which (46) follows.

Hence, we can ascertain that

$$\lim_{N \rightarrow \infty} 2^{-2N} \text{tr}_{B_1+B_2} \Omega(\sqrt{J_{\pm}J_{\mp}/N}, \sqrt{J_{\pm}J_{\mp}/N}) = 16 \int_0^{\infty} \int_0^{\infty} r s e^{-2(r^2+s^2)} \Omega(r, s) dr ds, \quad (49)$$

where $\Omega(r, s)$ is some complex-valued function for which the integrals on the right-hand side of equation (49) converge.

Using the above result, one can express the nonzero elements of the reduced density matrix corresponding to the initial state $\frac{1}{\sqrt{2}}(|-+\rangle - |+-\rangle)$, in the thermodynamic limit, as

$$\rho_{11}(t) = \rho_{44}(t) = \frac{1}{4}[\Lambda_+(t) + \Lambda_-(t)], \quad (50)$$

$$\rho_{22}(t) = \rho_{33}(t) = \frac{1}{4}[\Upsilon_+(t) + \Upsilon_-(t) + \Xi_+(t) + \Xi_-(t)], \quad (51)$$

$$\rho_{23}(t) = -\frac{1}{8}[\Upsilon_+(t) + \Upsilon_-(t) + \Xi_+(t) + \Xi_-(t) + 2\Psi(t)], \quad (52)$$

where (we set $\alpha = 1$ for the sake of shortness)

$$\Lambda_{\pm}(t) = 16 \int_0^{\infty} \int_0^{\infty} r s e^{-2(r^2+s^2)} \frac{(r \pm s)^2}{\delta^2 + (r \pm s)^2} \sin^2(t\sqrt{\delta^2 + (r \pm s)^2}) dr ds, \quad (53)$$

$$\Upsilon_{\pm}(t) = 16 \int_0^{\infty} \int_0^{\infty} r s e^{-2(r^2+s^2)} \cos^2(t\sqrt{\delta^2 + (r \pm s)^2}) dr ds, \quad (54)$$

$$\Xi_{\pm}(t) = 16 \int_0^{\infty} \int_0^{\infty} r s e^{-2(r^2+s^2)} \frac{\delta^2}{\delta^2 + (r \pm s)^2} \sin^2(t\sqrt{\delta^2 + (r \pm s)^2}) dr ds, \quad (55)$$

$$\begin{aligned} \Psi(t) &= 16 \int_0^{\infty} \int_0^{\infty} r s e^{-2(r^2+s^2)} \left\{ \cos(t\sqrt{\delta^2 + (r+s)^2}) \cos(t\sqrt{\delta^2 + (r-s)^2}) \right. \\ &\quad \left. + \delta^2 \frac{\sin(t\sqrt{\delta^2 + (r+s)^2}) \sin(t\sqrt{\delta^2 + (r-s)^2})}{\delta^2 + (r+s)^2} \frac{\sin(t\sqrt{\delta^2 + (r-s)^2})}{\delta^2 + (r-s)^2} \right\} dr ds. \end{aligned} \quad (56)$$

Unfortunately, the above functions cannot be evaluated analytically; one should have recourse to numerical integration. This task can be significantly simplified by transforming the double integration into a single one, which is much easier to carry out. To do that, note that a simple analysis of the expressions of the functions $\Lambda_{\pm}(t)$, $\Upsilon_{\pm}(t)$ and $\Xi_{\pm}(t)$ leads to the evaluation of the probability density functions $Q(\mu)$ and $R(\eta)$ corresponding, respectively, to the random variables $\mu = r + s$ and $\eta = r - s$ (see [31] for a similar situation). We show in appendix C that

$$Q(\mu) = [2\mu - \sqrt{\pi} e^{\mu^2} (1 - 2\mu^2) \operatorname{erf}(\mu)] e^{-2\mu^2}, \quad \mu \geq 0; \quad (57)$$

$$R(\eta) = \frac{1}{2} \{2|\eta| + \sqrt{\pi} e^{\eta^2} (1 - 2\eta^2) [1 - \operatorname{erf}(|\eta|)]\} e^{-2\eta^2}, \quad \eta \in \Re. \quad (58)$$

Functions (53)–(55) can easily be expressed in terms of the functions $Q(\mu)$ and $R(\eta)$. For example, we have

$$\Lambda_+(t) = \int_0^\infty Q(\mu) \frac{\mu^2}{\delta^2 + \mu^2} \sin^2(t\sqrt{\delta^2 + \mu^2}) d\mu, \quad (59)$$

$$\Lambda_-(t) = \int_{-\infty}^\infty R(\eta) \frac{\eta^2}{\delta^2 + \eta^2} \sin^2(t\sqrt{\delta^2 + \eta^2}) d\eta. \quad (60)$$

It should be noted that in contrast to r and s , the random variables η and μ are not independent. The function $\Psi(t)$ cannot be further simplified and should be evaluated using the double integration over the variables r and s . Nevertheless, using the Riemann–Lebesgue lemma, we can infer that

$$\lim_{t \rightarrow \infty} \Psi(t) = \Psi(\infty) = 0. \quad (61)$$

We find in a similar way that the remaining functions tend asymptotically to

$$\Lambda_+(\infty) = \frac{1}{2} \int_0^\infty Q(\mu) \frac{\mu^2}{\delta^2 + \mu^2} d\mu, \quad (62)$$

$$\Lambda_-(\infty) = \frac{1}{2} \int_{-\infty}^\infty R(\mu) \frac{\mu^2}{\delta^2 + \mu^2} d\mu, \quad (63)$$

$$\Upsilon_{\pm}(\infty) = \frac{1}{2}, \quad (64)$$

$$\Xi_+(\infty) = \frac{1}{2} \int_0^\infty Q(\mu) \frac{\delta^2}{\delta^2 + \mu^2} d\mu, \quad (65)$$

$$\Xi_-(\infty) = \frac{1}{2} \int_{-\infty}^\infty R(\mu) \frac{\delta^2}{\delta^2 + \mu^2} d\mu. \quad (66)$$

Note that

$$\Lambda_{\pm}(\infty) + \Xi_{\pm}(\infty) = \frac{1}{2}, \quad (67)$$

independent of the values of δ . It follows that the asymptotic density matrix can be expressed as

$$\rho(\infty) = \begin{pmatrix} \frac{\Pi}{4} & 0 & 0 & 0 \\ 0 & \frac{2-\Pi}{4} & -\frac{2-\Pi}{8} & 0 \\ 0 & -\frac{2-\Pi}{8} & \frac{2-\Pi}{4} & 0 \\ 0 & 0 & 0 & \frac{\Pi}{4} \end{pmatrix}, \tag{68}$$

where

$$\Pi = \Lambda_+(\infty) + \Lambda_-(\infty). \tag{69}$$

Before we study the general case, let us have a look at the two extreme cases: $\delta = 0$ and $\delta = \infty$. It is easily seen from equations (62)–(66) that

$$\lim_{\delta \rightarrow 0} \Xi_{\pm}(\infty) = 0, \quad \lim_{\delta \rightarrow 0} \Lambda_{\pm}(\infty) = \frac{1}{2}. \tag{70}$$

The corresponding asymptotic reduced density matrix reads as

$$\rho(\infty)_{\delta=0} = \begin{pmatrix} \frac{1}{4} & 0 & 0 & 0 \\ 0 & \frac{1}{4} & -\frac{1}{8} & 0 \\ 0 & -\frac{1}{8} & \frac{1}{4} & 0 \\ 0 & 0 & 0 & \frac{1}{4} \end{pmatrix}, \tag{71}$$

which has a concurrence and a purity identically equal to zero and $9/32$, respectively. In contrast, in the limit of strong coupling between the central qubits,

$$\lim_{\delta \rightarrow \infty} \Xi_{\pm}(\infty) = \frac{1}{2}, \quad \lim_{\delta \rightarrow \infty} \Lambda_{\pm}(\infty) = 0. \tag{72}$$

Consequently,

$$\rho(\infty)_{\delta=\infty} = \begin{pmatrix} 0 & 0 & 0 & 0 \\ 0 & \frac{1}{2} & -\frac{1}{4} & 0 \\ 0 & -\frac{1}{4} & \frac{1}{2} & 0 \\ 0 & 0 & 0 & 0 \end{pmatrix}. \tag{73}$$

A straightforward calculation shows that

$$\lim_{\delta \rightarrow \infty} C(\rho(\infty)) = \frac{1}{2}, \quad \lim_{\delta \rightarrow \infty} P(\rho(\infty)) = \frac{5}{8}. \tag{74}$$

We observe that the asymptotic concurrence and purity obtained here coincide, when $\delta \rightarrow \infty$, with those obtained for the states $|v_{\pm}\rangle$ in the case of a common spin bath. They are however different from the asymptotic values corresponding to the state $|e_+\rangle$ which are identically equal to 1 (the state $|e_-\rangle$ is stationary).

In general, since $0 \leq \mu^2/(\mu^2 + \delta^2) \leq 1$, then

$$\begin{aligned} 0 \leq \Pi &= \frac{1}{2} \int_0^{\infty} Q(\mu) \frac{\mu^2}{\delta^2 + \mu^2} d\mu + \frac{1}{2} \int_{-\infty}^{\infty} R(\mu) \frac{\mu^2}{\delta^2 + \mu^2} d\mu \\ &\leq \frac{1}{2} \int_0^{\infty} Q(\mu) d\mu + \frac{1}{2} \int_{-\infty}^{\infty} R(\mu) d\mu = 1. \end{aligned} \tag{75}$$

This allows us to find the following explicit form of the asymptotic value of the concurrence:

$$C(\infty) = \max \left\{ 0, \frac{2-3\Pi}{4} \right\}. \tag{76}$$

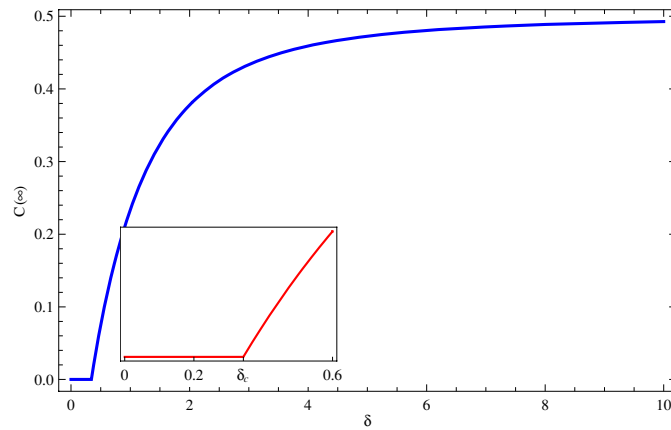


Figure 3. The variation of $C(\infty)$ as a function of the coupling constant δ . The inset shows the critical point δ_c . α is set to 1.

The latter can also be rewritten as

$$C(\infty) = \begin{cases} \frac{2 - 3\Pi}{4} & \text{for } 0 \leq \Pi \leq \frac{2}{3}, \\ 0 & \text{for } \frac{2}{3} \leq \Pi \leq 1. \end{cases} \quad (77)$$

The variation of the asymptotic concurrence as a function of δ is shown in figure 3. It can be seen that $C(\infty)$ remains zero up to a critical value δ_c after which it increases, to tend asymptotically to $\frac{1}{2}$. The value of δ_c can be evaluated numerically:

$$\delta_c = 0.342\ 842, \quad \Pi|_{\delta=\delta_c} = 0.666\ 666. \quad (78)$$

At the critical point, the density matrix reads as

$$\rho_c(\infty) = \begin{pmatrix} \frac{1}{6} & 0 & 0 & 0 \\ 0 & \frac{1}{3} & -\frac{1}{6} & 0 \\ 0 & -\frac{1}{6} & \frac{1}{3} & 0 \\ 0 & 0 & 0 & \frac{1}{6} \end{pmatrix}, \quad (79)$$

and hence $P(\rho_c(\infty)) = \frac{1}{3}$.

6. Second-order master equation

The aim of this section is to study the short-time behaviour of the dynamics. This will be achieved by investigating the second-order master equation under Born approximation. In the interaction picture, the above yield the following set of integro-differential equations:

$$\dot{\tilde{\rho}}_{11}(t) = -\alpha^2 \int_0^t (2\tilde{\rho}_{11}(s) - \tilde{\rho}_{22}(s) - \tilde{\rho}_{33}(s)) \cos[2\delta(t-s)] ds, \quad (80)$$

$$\dot{\tilde{\rho}}_{12}(t) = -\alpha^2 \int_0^t (2\tilde{\rho}_{12}(s) e^{2i\delta(t-s)} - \tilde{\rho}_{34}(s) e^{2i\delta(t+s)}) ds, \quad (81)$$

$$\dot{\tilde{\rho}}_{13}(t) = -\alpha^2 \int_0^t (2\tilde{\rho}_{13}(s) e^{2i\delta(t-s)} - \tilde{\rho}_{24}(s) e^{2i\delta(t+s)}) ds, \quad (82)$$

$$\dot{\tilde{\rho}}_{14}(t) = -\alpha^2 \int_0^t 2\tilde{\rho}_{13}(s) \cos[2\delta(t-s)] ds, \tag{83}$$

$$\dot{\tilde{\rho}}_{22}(t) = -\alpha^2 \int_0^t (2\tilde{\rho}_{22}(s) - \tilde{\rho}_{11}(s) - \tilde{\rho}_{44}(s)) \cos[2\delta(t-s)] ds, \tag{84}$$

$$\dot{\tilde{\rho}}_{23}(t) = -\alpha^2 \int_0^t 2\tilde{\rho}_{23}(s) \cos[2\delta(t-s)] ds, \tag{85}$$

$$\dot{\tilde{\rho}}_{24}(t) = -\alpha^2 \int_0^t (2\tilde{\rho}_{24}(s) e^{2i\delta(s-t)} - \tilde{\rho}_{13}(s) e^{-2i\delta(t+s)}) ds, \tag{86}$$

$$\dot{\tilde{\rho}}_{33}(t) = -\alpha^2 \int_0^t (2\tilde{\rho}_{33}(s) - \tilde{\rho}_{11}(s) - \tilde{\rho}_{44}(s)) \cos[2\delta(t-s)] ds, \tag{87}$$

$$\dot{\tilde{\rho}}_{34}(t) = -\alpha^2 \int_0^t (2\tilde{\rho}_{34}(s) e^{2i\delta(s-t)} - \tilde{\rho}_{12}(s) e^{-2i\delta(t+s)}) ds, \tag{88}$$

$$\dot{\tilde{\rho}}_{44}(t) = -\alpha^2 \int_0^t (2\tilde{\rho}_{44}(s) - \tilde{\rho}_{22}(s) - \tilde{\rho}_{33}(s)) \cos[2\delta(t-s)] ds. \tag{89}$$

Here the tilde designates the interaction picture, namely $\tilde{\rho}(t) = e^{iH_0 t} \rho(t) e^{-iH_0 t}$. It is worth mentioning that the integro-differential equations corresponding to the off-diagonal elements (except ρ_{13}) obtained from the second-order master equation in [27] are somewhat wrong; the matrix elements under the integral sign are, in fact, expressed in the Schrödinger picture.

Clearly, the above equations do not depend on the number of spins within the bath. In fact it is found that at short times, the exact solution discussed in the precedent sections give the same result with fixed δ no matter what the value of N . This explains the results of [25–27]. Of course, the solutions quickly diverge from each other as we increase the time.

Equations (80)–(89) can be solved under a time-local approximation in which the matrix elements $\tilde{\rho}_{ij}(s)$ are replaced by $\tilde{\rho}_{ij}(t)$. One can find that (α is set to 1)

$$\begin{aligned} \tilde{\rho}_{11}(t) = & \frac{1}{4} \left\{ 1 + [-1 + 2(\rho_{11}^0 + \rho_{44}^0)] \exp \left\{ \frac{1}{\delta^2} [\cos(2\delta t) - 1] \right\} \right. \\ & \left. + 2(\rho_{11}^0 - \rho_{44}^0) \exp \left\{ \frac{1}{2\delta^2} [\cos(2\delta t) - 1] \right\} \right\}, \end{aligned} \tag{90}$$

$$\begin{aligned} \tilde{\rho}_{22}(t) = & \frac{1}{4} \left\{ 1 + [-1 + 2(\rho_{22}^0 + \rho_{33}^0)] \exp \left\{ \frac{1}{\delta^2} [\cos(2\delta t) - 1] \right\} \right. \\ & \left. + 2(\rho_{22}^0 - \rho_{33}^0) \exp \left\{ \frac{1}{2\delta^2} [\cos(2\delta t) - 1] \right\} \right\}, \end{aligned} \tag{91}$$

$$\begin{aligned} \tilde{\rho}_{33}(t) = & \frac{1}{4} \left\{ 1 + [-1 + 2(\rho_{33}^0 + \rho_{22}^0)] \exp \left\{ \frac{1}{\delta^2} [\cos(2\delta t) - 1] \right\} \right. \\ & \left. + 2(\rho_{33}^0 - \rho_{22}^0) \exp \left\{ \frac{1}{2\delta^2} [\cos(2\delta t) - 1] \right\} \right\}, \end{aligned} \tag{92}$$

$$\begin{aligned} \tilde{\rho}_{44}(t) = & \frac{1}{4} \left\{ 1 + [-1 + 2(\rho_{44}^0 + \rho_{11}^0)] \exp \left\{ \frac{1}{\delta^2} [\cos(2\delta t) - 1] \right\} \right. \\ & \left. + 2(\rho_{44}^0 - \rho_{11}^0) \exp \left\{ \frac{1}{2\delta^2} [\cos(2\delta t) - 1] \right\} \right\}, \end{aligned} \tag{93}$$

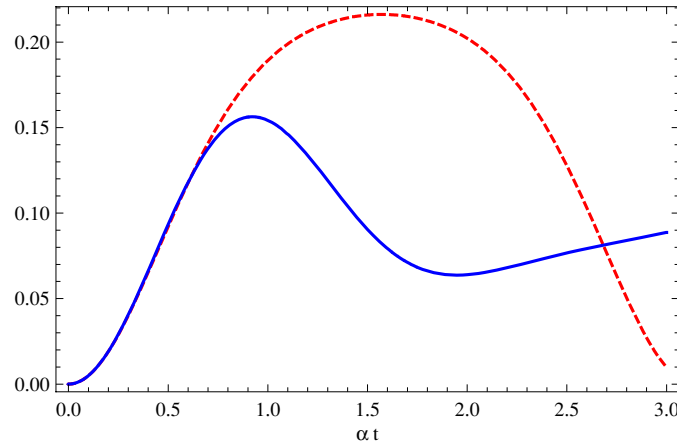


Figure 4. The variation in time of the matrix element $\rho_{11}(t)$ corresponding to the singlet state. The solid curve represents the exact solution and the dashed curve represents the approximate solution (90). The parameters are $N = 10$ and $\delta = \alpha$.

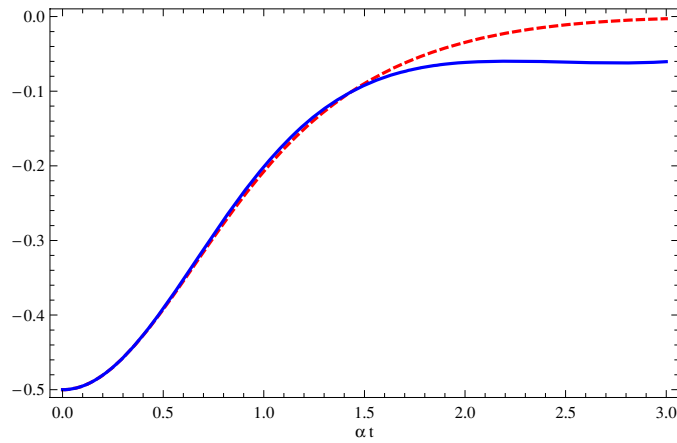


Figure 5. The variation in time of the matrix element $\rho_{12}(t)$ corresponding to the singlet state. The solid curve represents the exact solution and the dashed curve represents the approximate solution (97). The parameters are $N = 10$ and $\delta = 0$.

$$\tilde{\rho}_{14}(t) = \rho_{14}^0 \exp \left\{ \frac{1}{\delta^2} [\cos(2\delta t) - 1] \right\}, \tag{94}$$

$$\tilde{\rho}_{23}(t) = \rho_{23}^0 \exp \left\{ \frac{1}{\delta^2} [\cos(2\delta t) - 1] \right\}. \tag{95}$$

These solutions describe approximately the dynamics at short times (see figure 4). In fact, the smaller the coupling constant δ , the better these solutions are.

When $\delta = 0$ (i.e. nonlocal dynamics), then

$$\exp \left\{ \frac{1}{n\delta^2} [\cos(2\delta t) - 1] \right\} \rightarrow e^{-2t^2/n}, \quad n = 1, 2. \tag{96}$$

Thus, the second-order time-local master equation shows that the nonlocal dynamics or, in general, the short-time behaviour follow a Gaussian decay law. Note that the solutions

corresponding to the diagonal elements reproduce the asymptotic values for $N \rightarrow \infty$, namely $\rho_{ii}(\infty) = \frac{1}{4}$. However, those corresponding to the off-diagonal elements fail to reproduce the steady state, since, for example, equation (95) implies that $\rho_{23}(t) \rightarrow 0$. To end our discussion, let us remark that equations (81), (82), (86) and (88) can be analytically solved only when $\delta = 0$. For instance (see figure 5),

$$\rho_{12}(t) = \frac{1}{2}[(\rho_{12}^0 + \rho_{34}^0) e^{-t^2/2} + (\rho_{12}^0 - \rho_{34}^0) e^{-3t^2/2}]. \tag{97}$$

7. Summary

In summary, we have investigated the dynamics of two qubits coupled to separate spin star environments via Heisenberg XY interactions. We have derived the exact form of the time evolution operator and calculated the matrix elements of the reduced density operator. The analysis of the evolution in time of the concurrence and the purity shows that decoherence can be minimized by allowing the central qubits to strongly interact with each other. The short-time behaviour, studied by deriving the second-order master equation, is found to be Gaussian. The next step may consist in considering more central qubits and investigate whether the above results still hold.

Acknowledgments

The author would like to thank the referees for their valuable suggestions.

Appendix A

It can be shown by induction that powers of $H_{S_1 B_1}$ and $H_{S_2 B_2}$ are given by

$$H_{S_1 B_1}^{2k} = \left(\frac{\alpha}{\sqrt{N}}\right)^{2k} \begin{pmatrix} (J_+ J_-)^k & 0 & 0 & 0 \\ 0 & (J_+ J_-)^k & 0 & 0 \\ 0 & 0 & (J_- J_+)^k & 0 \\ 0 & 0 & 0 & (J_- J_+)^k \end{pmatrix}, \tag{A.1}$$

$$H_{S_1 B_1}^{2k+1} = \left(\frac{\alpha}{\sqrt{N}}\right)^{2k+1} \begin{pmatrix} 0 & 0 & J_+(J_- J_+)^k & 0 \\ 0 & 0 & 0 & J_+(J_- J_+)^k \\ J_-(J_+ J_-)^k & 0 & 0 & 0 \\ 0 & J_-(J_+ J_-)^k & 0 & 0 \end{pmatrix}, \tag{A.2}$$

$$H_{S_2 B_2}^{2k} = \left(\frac{\alpha}{\sqrt{N}}\right)^{2k} \begin{pmatrix} (J_+ J_-)^k & 0 & 0 & 0 \\ 0 & (J_- J_+)^k & 0 & 0 \\ 0 & 0 & (J_+ J_-)^k & 0 \\ 0 & 0 & 0 & (J_- J_+)^k \end{pmatrix}, \tag{A.3}$$

$$H_{S_2 B_2}^{2k+1} = \left(\frac{\alpha}{\sqrt{N}}\right)^{2k+1} \begin{pmatrix} 0 & J_+(J_- J_+)^k & 0 & 0 \\ J_-(J_+ J_-)^k & 0 & 0 & 0 \\ 0 & 0 & 0 & J_+(J_- J_+)^k \\ 0 & 0 & J_-(J_+ J_-)^k & 0 \end{pmatrix}. \tag{A.4}$$

On the other hand, the matrix elements of H^{2n+1} are given by

$$(H^{2n+1})_{11} = \frac{1}{2} \delta[(\mathcal{M}_1^+)^n + (\mathcal{M}_1^-)^n], \tag{A.5}$$

$$(H^{2n+1})_{12} = \mathcal{J}_+ \frac{\alpha}{2\sqrt{N\mathcal{J}_-\mathcal{J}_+}} [(\sqrt{\mathcal{J}_-\mathcal{J}_+} + \sqrt{J_+J_-})(\mathcal{M}_2^+)^n \tag{A.6}$$

$$+ (\sqrt{\mathcal{J}_-\mathcal{J}_+} - \sqrt{J_+J_-})(\mathcal{M}_2^-)^n], \tag{A.7}$$

$$(H^{2n+1})_{13} = J_+ \frac{\alpha}{2\sqrt{N\mathcal{J}_-\mathcal{J}_+}} [(\sqrt{\mathcal{J}_+\mathcal{J}_-} + \sqrt{J_-J_+})(\mathcal{M}_3^+)^n \tag{A.8}$$

$$+ (\sqrt{J_-J_+} - \sqrt{\mathcal{J}_+\mathcal{J}_-})(\mathcal{M}_3^-)^n], \tag{A.9}$$

$$(H^{2n+1})_{14} = (\delta/2)J_+\mathcal{J}_+ \frac{(\mathcal{M}_4^+)^n - (\mathcal{M}_4^-)^n}{\sqrt{J_-J_+\mathcal{J}_-\mathcal{J}_+}}, \tag{A.10}$$

$$(H^{2n+1})_{21} = \mathcal{J}_- \frac{\alpha}{2\sqrt{N\mathcal{J}_+\mathcal{J}_-}} [(\sqrt{\mathcal{J}_+\mathcal{J}_-} + \sqrt{J_+J_-})(\mathcal{M}_1^+)^n \tag{A.11}$$

$$+ (\sqrt{\mathcal{J}_+\mathcal{J}_-} - \sqrt{J_+J_-})(\mathcal{M}_1^-)^n], \tag{A.12}$$

$$(H^{2n+1})_{22} = -\frac{1}{2}\delta[(\mathcal{M}_2^+)^n + (\mathcal{M}_2^-)^n], \tag{A.13}$$

$$(H^{2n+1})_{23} = -(\delta/2)J_+\mathcal{J}_- \frac{(\mathcal{M}_3^+)^n - (\mathcal{M}_3^-)^n}{\sqrt{J_-J_+\mathcal{J}_+\mathcal{J}_-}}, \tag{A.14}$$

$$(H^{2n+1})_{24} = J_+ \frac{\alpha/2}{\sqrt{N\mathcal{J}_-\mathcal{J}_+}} [(\sqrt{\mathcal{J}_-\mathcal{J}_+} + \sqrt{J_-J_+})(\mathcal{M}_4^+)^n \tag{A.15}$$

$$+ (\sqrt{J_-J_+} - \sqrt{\mathcal{J}_-\mathcal{J}_+})(\mathcal{M}_4^-)^n], \tag{A.16}$$

$$(H^{2n+1})_{31} = J_- \frac{\alpha/2}{\sqrt{N\mathcal{J}_+\mathcal{J}_-}} [(\sqrt{J_+J_-} + \sqrt{\mathcal{J}_+\mathcal{J}_-})(\mathcal{M}_1^+)^n \tag{A.17}$$

$$+ (\sqrt{J_+J_-} - \sqrt{\mathcal{J}_+\mathcal{J}_-})(\mathcal{M}_1^-)^n], \tag{A.18}$$

$$(H^{2n+1})_{32} = -(\delta/2)J_-\mathcal{J}_+ \frac{(\mathcal{M}_2^+)^n - (\mathcal{M}_2^-)^n}{\sqrt{J_+J_-\mathcal{J}_-\mathcal{J}_+}}, \tag{A.19}$$

$$(H^{2n+1})_{33} = -\frac{1}{2}\delta[(\mathcal{M}_3^+)^n + (\mathcal{M}_3^-)^n], \tag{A.20}$$

$$(H^{2n+1})_{34} = \mathcal{J}_+ \frac{\alpha/2}{\sqrt{N\mathcal{J}_-\mathcal{J}_+}} [(\sqrt{\mathcal{J}_-\mathcal{J}_+} + \sqrt{J_-J_+})(\mathcal{M}_4^+)^n \tag{A.21}$$

$$+ (\sqrt{\mathcal{J}_-\mathcal{J}_+} - \sqrt{J_-J_+})(\mathcal{M}_4^-)^n], \tag{A.22}$$

$$(H^{2n+1})_{41} = (\delta/2)J_-\mathcal{J}_- \frac{(\mathcal{M}_1^+)^n - (\mathcal{M}_1^-)^n}{\sqrt{J_+J_-\mathcal{J}_+\mathcal{J}_-}}, \tag{A.23}$$

$$(H^{2n+1})_{42} = J_- \frac{\alpha/2}{\sqrt{N\mathcal{J}_+\mathcal{J}_-}} [(\sqrt{\mathcal{J}_-\mathcal{J}_+} + \sqrt{J_+J_-})(\mathcal{M}_2^+)^n \tag{A.24}$$

$$+ (\sqrt{J_+J_-} - \sqrt{\mathcal{J}_-\mathcal{J}_+})(\mathcal{M}_2^-)^n], \tag{A.25}$$

$$(H^{2n+1})_{43} = \mathcal{J}_- \frac{\alpha/2}{\sqrt{N\mathcal{J}_+\mathcal{J}_-}} [(\sqrt{\mathcal{J}_+\mathcal{J}_-} + \sqrt{J_-J_+})(\mathcal{M}_3^+)^n \tag{A.26}$$

$$+ (\sqrt{\mathcal{J}_+\mathcal{J}_-} - \sqrt{J_-J_+})(\mathcal{M}_3^-)^n], \tag{A.27}$$

$$(H^{2n+1})_{44} = \frac{1}{2}\delta[(\mathcal{M}_4^+)^n + (\mathcal{M}_4^-)^n]. \tag{A.28}$$

Appendix B

Using trace properties of the lowering and raising operators, it can be shown that the nonzero matrix elements corresponding to the initial maximally entangled states $\frac{1}{\sqrt{2}}(|- +\rangle \pm |+ -\rangle)$ are explicitly given by

$$\rho_{11}(t) = 2^{-(2N+1)} \text{tr}_{B_1+B_2} \{U_{12}(t)U_{12}^\dagger(t) + U_{13}(t)U_{13}^\dagger(t)\}, \tag{B.1}$$

$$\rho_{22}(t) = 2^{-(2N+1)} \text{tr}_{B_1+B_2} \{U_{22}(t)U_{22}^\dagger(t) + U_{23}(t)U_{23}^\dagger(t)\}, \tag{B.2}$$

$$\rho_{23}(t) = \pm 2^{-(2N+1)} \text{tr}_{B_1+B_2} \{U_{22}(t)U_{33}^\dagger(t)\}, \tag{B.3}$$

$$\rho_{33}(t) = 2^{-(2N+1)} \text{tr}_{B_1+B_2} \{U_{32}(t)U_{32}^\dagger(t) + U_{33}(t)U_{33}^\dagger(t)\}, \tag{B.4}$$

$$\rho_{44}(t) = 2^{-(2N+1)} \text{tr}_{B_1+B_2} \{U_{42}(t)U_{42}^\dagger(t) + U_{43}(t)U_{43}^\dagger(t)\}. \tag{B.5}$$

Those associated with the initial state $\frac{1}{\sqrt{2}}(|- -\rangle \pm |+ +\rangle)$ read as

$$\rho_{11}(t) = 2^{-(2N+1)} \text{tr}_{B_1+B_2} \{U_{11}(t)U_{11}^\dagger(t) + U_{14}(t)U_{14}^\dagger(t)\}, \tag{B.6}$$

$$\rho_{22}(t) = 2^{-(2N+1)} \text{tr}_{B_1+B_2} \{U_{21}(t)U_{21}^\dagger(t) + U_{24}(t)U_{24}^\dagger(t)\}, \tag{B.7}$$

$$\rho_{14}(t) = \pm 2^{-(2N+1)} \text{tr}_{B_1+B_2} \{U_{11}(t)U_{44}^\dagger(t)\}, \tag{B.8}$$

$$\rho_{33}(t) = 2^{-(2N+1)} \text{tr}_{B_1+B_2} \{U_{31}(t)U_{31}^\dagger(t) + U_{34}(t)U_{34}^\dagger(t)\}, \tag{B.9}$$

$$\rho_{44}(t) = 2^{-(2N+1)} \text{tr}_{B_1+B_2} \{U_{41}(t)U_{41}^\dagger(t) + U_{44}(t)U_{44}^\dagger(t)\}. \tag{B.10}$$

Appendix C

In this appendix, we derive the probability density functions $Q(\mu)$ and $R(\eta)$. Let us begin with the random variable μ ; its probability density function is simply given by the convolution of $f(r)$ with itself:

$$Q(\mu) = 16 \int_0^\mu (\mu - r)r e^{-2(\mu-r)^2-2r^2} dr. \tag{C.1}$$

Note that the upper limit of the integration over r is μ because the quantity $\mu - r$ should be positive. The evaluation of the integral is somewhat lengthy, but elementary; the result is given by equation (57), with $\text{erf}(x)$ designating the error function [32].

Now consider the variable $\eta = r - s$. One should be careful when using the definition of the convolution, since, in this case, η belongs to the interval $]-\infty, \infty[$. We have to distinguish between two cases, namely $\eta \geq 0$ and $\eta \leq 0$. In the first case $r \in [0, \infty[$, and hence

$$\begin{aligned} R(\eta \geq 0) &= 16 \int_0^\infty (\eta + r)r e^{-2(r+s)^2-2r^2} dr \\ &= \frac{1}{2} \{2\eta + \sqrt{\pi} e^{\eta^2} (1 - 2\eta^2)[1 - \text{erf}(\eta)]\} e^{-2\eta^2}. \end{aligned} \tag{C.2}$$

When $\eta \leq 0$, then $r \in [-\eta, \infty[$, which implies that

$$\begin{aligned} R(\eta \leq 0) &= 16 \int_{-\eta}^\infty (\eta + r)r e^{-2(r+s)^2-2r^2} dr \\ &= \frac{1}{2} \{-2\eta + \sqrt{\pi} e^{\eta^2} (1 - 2\eta^2)[1 + \text{erf}(\eta)]\} e^{-2\eta^2}. \end{aligned} \tag{C.3}$$

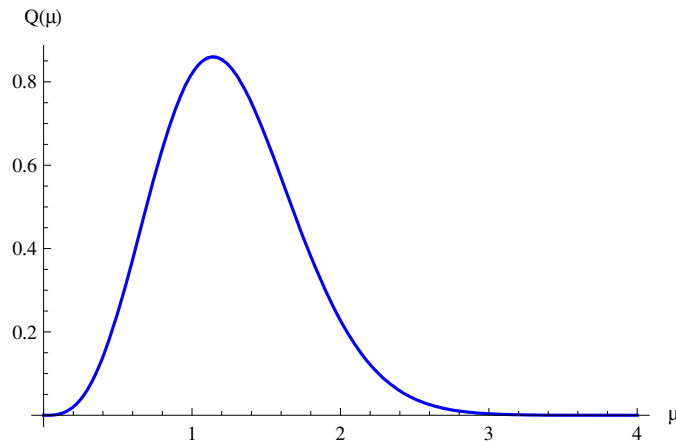


Figure 1. The probability density function $Q(\mu)$.

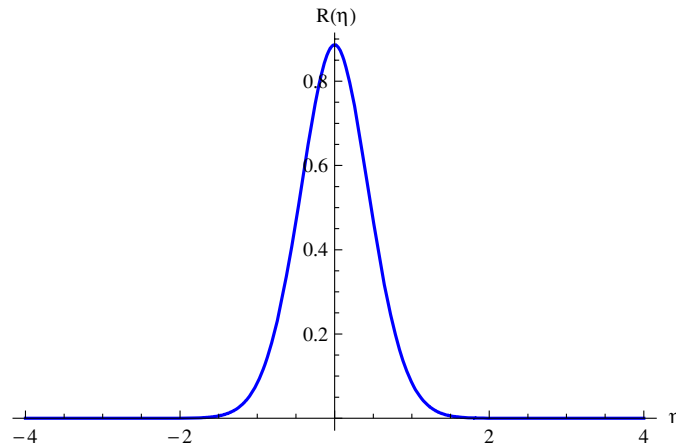


Figure 2. The probability density function $R(\eta)$.

Combining (C.2) and (C.3), we obtain the expression for the probability density function of η over the real line displayed in equation (58)

The above functions are depicted in figures 1 and 2. Clearly, $R(\eta)$ is an even function of its argument; it takes its maximum value at the origin, that is, $\max\{R(\eta)\} = R(0) = 0.886\ 227$. The maximum value of $Q(\mu)$ occurs at $\mu_0 = 1.142\ 088$, such that $\max\{Q(\mu)\} = Q(\mu_0) = 0.859\ 664$.

As a simple application, let us prove the following.

Theorem 1. *The moments around the origin of the random variables μ and η are given by*

$$\langle \mu^{2n} \rangle = \frac{n!}{2^n} \left[1 + 2^{n+1} n {}_2F_1 \left(1 + n, \frac{1}{2}; \frac{3}{2}; -1 \right) \right], \tag{C.4}$$

$$\langle \mu^{2n+1} \rangle = \frac{\Gamma(\frac{3}{2} + n)}{2^n} \left[\frac{1}{\sqrt{2}} + 2^n (2n + 1) {}_2F_1 \left(\frac{3}{2} + n, \frac{1}{2}; \frac{3}{2}; -1 \right) \right], \tag{C.5}$$

$$\langle \eta^{2n} \rangle = \langle \mu^{2n} \rangle - n\sqrt{\pi}\Gamma\left(\frac{1}{2} + n\right), \tag{C.6}$$

$$\langle \eta^{2n+1} \rangle = 0, \tag{C.7}$$

where $\Gamma(x)$ and ${}_2F_1(a, b; c; d)$ denote the Gamma and the hypergeometric functions, respectively.

Proof. Relation (C.7) is obvious since the function $R(\eta)$ is even. Let us prove (C.4). We have that

$$\begin{aligned} \langle \mu^{2n} \rangle &= \int_0^\infty \mu^{2n} Q(\mu) d\mu \\ &= 2I_{n+1} - I_n + 2Y_n, \end{aligned} \tag{C.8}$$

where

$$I_n = \int_0^\infty \sqrt{\pi} \mu^{2n} e^{-\mu^2} \operatorname{erf}(\mu) d\mu, \tag{C.9}$$

$$Y_n = \int_0^\infty \mu^{2n+1} e^{-2\mu^2} d\mu. \tag{C.10}$$

To calculate Y_n and I_n , introduce the functions of the real variable $x > 0$:

$$Y_n(x) = \int_0^\infty \mu^{2n+1} e^{-\mu^2(1+\frac{1}{x})} d\mu, \tag{C.11}$$

$$I_n(x) = \int_0^\infty \sqrt{\pi} \mu^{2n} e^{-\mu^2/x} \operatorname{erf}(\mu) d\mu. \tag{C.12}$$

The first integral can be easily evaluated:

$$Y_n(x) = \frac{1}{2} \left(\frac{x}{1+x}\right)^{n+1} \int_0^\infty \chi^n e^{-\chi} d\chi = \frac{n!}{2} \left(\frac{x}{1+x}\right)^{n+1}. \tag{C.13}$$

The second integral satisfies

$$\frac{dI_n(x)}{dx} = \frac{1}{x^2} I_{n+1}(x). \tag{C.14}$$

Integrating by parts the rhs of (C.12) with respect to μ and using (C.13) yield

$$I_{n+1}(x) = \frac{x(2n+1)}{2} I_n(x) + \frac{xn!}{2} \left(\frac{x}{x+1}\right)^{n+1}. \tag{C.15}$$

Here, we have used the fact that $\operatorname{erf}(x)' = 2e^{-x^2}/\sqrt{\pi}$.

Let $I_n(x) = n!x^{n+1}g_n(x)$. Then from (C.15), we have

$$2(n+1)g_{n+1}(x) = (2n+1)g_n(x) + \frac{1}{(x+1)^{n+1}}. \tag{C.16}$$

On the other hand, equation (C.14) implies that

$$x \frac{dg_n(x)}{dx} + (n+1)g_n(x) = (n+1)g_{n+1}(x). \tag{C.17}$$

Combining the last two equations yields the following first-order differential equation for the function $g_n(x)$:

$$2x \frac{dg_n(x)}{dx} + g_n(x) - \frac{1}{(x+1)^{n+1}} = 0. \tag{C.18}$$

Differentiating both sides of (C.18), and again using (C.16), we obtain

$$\left[\frac{d^2}{dx^2} + \left(\frac{3}{2x} + \frac{n+1}{x+1} \right) \frac{d}{dx} + \frac{n+1}{2x(x+1)} \right] g_n(x) = 0. \quad (\text{C.19})$$

By setting $y = -x$ and $h_n(y) = g_n(-x)$, we obtain

$$\left[\frac{d^2}{dy^2} + \left(\frac{3}{2y} + \frac{n+1}{y-1} \right) \frac{d}{dy} + \frac{n+1}{2y(y-1)} \right] h_n(y) = 0, \quad (\text{C.20})$$

which should be compared with the hypergeometric equation

$$\left[\frac{d^2}{dy^2} + \left(\frac{c}{y} + \frac{1+a+b-c}{y-1} \right) \frac{d}{dy} + \frac{ab}{y(y-1)} \right] {}_2F_1(a, b; c; y) = 0. \quad (\text{C.21})$$

Thus,

$$a = n+1, \quad b = \frac{1}{2}, \quad c = \frac{3}{2}. \quad (\text{C.22})$$

It follows that

$$I_n(x) = n! x^{n+1} {}_2F_1\left(n+1, \frac{1}{2}; \frac{3}{2}; -x\right). \quad (\text{C.23})$$

Putting $x = 1$ yields

$$I_n = n! {}_2F_1\left(n+1, \frac{1}{2}; \frac{3}{2}; -1\right), \quad Y_n = \frac{n!}{2^{n+2}}. \quad (\text{C.24})$$

Also, using (C.15), we obtain

$$2I_{n+1} = (2n+1)n! {}_2F_1\left(n+1, \frac{1}{2}; \frac{3}{2}; -1\right) + \frac{n!}{2^{n+1}}, \quad (\text{C.25})$$

from which (C.4) readily follows. The other moments can be evaluated with a similar method. \square

References

- [1] Baxter R J 1982 *Exactly Solved Models in Statistical Mechanics* (London: Academic)
- [2] Breuer H P and Petruccione F 2002 *The Theory of Open Quantum Systems* (Oxford: Oxford University Press)
- [3] Zurek W H 1991 *Phys. Today* **44** 36
- [4] DiVincenzo D P and Loss D 2000 *J. Magn. Magn. Matter* **200** 202
- [5] Zurek W H 2003 *Rev. Mod. Phys.* **75** 715–75
- [6] Nielsen M A and Chuang I L 2000 *Quantum Computation and Quantum Information* (Cambridge: Cambridge University Press)
- [7] Bennett C H and Wiesner S J 1993 *Phys. Rev. Lett.* **69** 2881
- [8] Bennett C H and DiVincenzo D P 2000 *Nature* **404** 247
- [9] Bennett C H, Brassard G, Crépau C, Jozsa R, Peres A and Wootters W K 1993 *Phys. Rev. Lett.* **70** 1895
- [10] Bennett C H, DiVincenzo D P, Smolin J A and Wootters W K 1996 *Phys. Rev. A* **54** 3824
- [11] Lloyd S 1993 *Science* **261** 1569
- [12] Ekert A and Jozsa R 1998 *Phil. Trans. R. Soc. A* **356** 1769
- [13] Loss D and DiVincenzo D P 1998 *Phys. Rev. A* **57** 120
- [14] Burkard G, Loss D and DiVincenzo D P 1999 *Phys. Rev. B* **59** 2070
- [15] Prokof'ev N V and Stamp P C E 2000 *Rep. Prog. Phys.* **63** 669
- [16] Zhang W, Dobrovitski V V, Al-Hassanieh K A, Dagotto E and Harmon B N 2006 *Phys. Rev. B* **74** 205313
- [17] Amico L, Fazio R, Osterloh A and Vedral V 2008 *Rev. Mod. Phys.* **80** 517
- [18] Gedik Z 2006 *Solid State Commun.* **138** 82
- [19] Coish W A and Loss D 2005 *Phys. Rev. B* **72** 125337
- [20] Hutton A and Bose S 2004 *Phys. Rev. A* **69** 042312
- [21] Breuer H P, Burgarth D and Petruccione F 2004 *Phys. Rev. B* **70** 045323
- [22] Yuan X Z, Goan H J and Zhu K D 2007 *Phys. Rev. B* **75** 045331

- [23] Jing J and Lü Z 2007 *Phys. Rev. B* **75** 174425
- [24] Jing J, Lü Z and Yang G 2007 *Phys. Rev. A* **76** 032322
- [25] Hamdouni Y and Petruccione F 2007 *Phys. Rev. B* **76** 174306
- [26] Hamdouni Y, Fannes M and Petruccione F 2006 *Phys. Rev. B* **73** 245323
- [27] Hamdouni Y 2007 *J. Phys. A: Math. Theor.* **40** 11569
- [28] Von Waldenfels W 1990 *Séminaire de probabilité (Starsburg) tome vol 24* (Berlin: Springer) pp 349–56
- [29] Wootters W K 1998 *Phys. Rev. Lett.* **80** 2245
- [30] Yu T and Eberly J H 2004 *Phys. Rev. Lett.* **93** 140404
- [31] Hamdouni Y 2009 *Phys. Lett. A* **373** 1233 (arXiv:0807.3944v2)
- [32] Danos M and Rafelski J 1984 *Pocketbook of Mathematical Functions* (Frankfurt: H Deutsch)